A comparative study of static, continuous, and dynamic calibration methods for high-precision low-force strain-gauge transducers

A comparative study of static, continuous, and dynamic calibration methods for high-precision low-force strain-gauge transducers

Andrea Prato[*], *Alessio Facello, Alessandro Germak, Alessandro Schiavi*

INRiM - Istituto Nazionale di Ricerca Metrologica, 10135 Torino, Italy

Corresponding author e-mail: *a.prato@inrim.it*

A comparative study of static, continuous, and dynamic calibration methods for high-precision low-force strain-gauge transducers

Abstract

The ISO 376 standard, which underpins static force calibration procedures, does not adequately address the time- and frequency-dependent effects encountered in real-world applications such as aerospace, automotive, and biomedical testing. This study investigates and compares static, continuous, and dynamic calibration methodologies applied to low-force strain-gauge transducers with capacities ranging from 50 N to 500 N. A 200 N transducer was calibrated using all three methods, while others were tested statically and dynamically. Static calibration yielded consistent sensitivity and low uncertainty across all force levels. Continuous calibration, based on DKD-R 3-9, produced comparable sensitivities but showed increased uncertainty, primarily due to reversibility effects and mechanical coupling imperfections. Dynamic calibration, conducted per DKD-R 3-10 using sinusoidal excitation, revealed a frequency-dependent sensitivity reduction, with Monte Carlo-based regression models used to characterize performance. While results across all methods are broadly compatible within declared uncertainties, significant divergence emerges when uncertainties are reduced to static levels. This raises important questions about the traceability and comparability of force measurements under non-static conditions. The findings underscore the need for further refinement in continuous and dynamic calibration methods to meet the demands of advanced material and structural testing.

Keywords: force transducer; force calibration; static; continuous; dynamic.

1. Introduction

Mechanical and material testing play a vital role in a wide range of industrial domains, including aerospace, automotive, healthcare, and manufacturing, where product integrity, safety, and compliance are of critical importance. In these environments, force transducers are essential tools for measuring mechanical loads during both research and quality assurance processes. However, traditional force calibration methods are largely based on static loading scenarios, which do not accurately reflect the dynamic nature of many real-world applications. Effects linked to time- and frequency-dependent behavior are often neglected, undermining the metrological traceability and reliability of test data in dynamic use cases [1,2].

The existing ISO 376 standard [3] outlines detailed procedures for the static calibration of force transducers and is widely adopted for verifying uniaxial testing machines. However, as the use of force transducers in high-rate and cyclic loading applications becomes increasingly common, the limitations of ISO 376 have become more evident. To meet these evolving needs, new calibration approaches have been developed to extend traceability to continuous and dynamic loading conditions. In this regard, two complementary guidelines have emerged: DKD-R 3-9 [4], which addresses continuous calibration using comparison methods, and DKD-R 3-10 (Sheet 2) [5], which provides procedures for dynamic calibration via sinusoidal excitation. These documents aim to close the methodological gap between static calibration standards and the demands of modern materials testing and structural dynamics.

In parallel with these efforts, the ComTraForce project (EURAMET 18SIB08) [6] has significantly contributed to the advancement of dynamic force calibration methods. The project focused on developing traceability solutions for force transducers operating under dynamic and continuous conditions. The project has delivered validated primary calibration setups, improved measurement uncertainty models, and tested the applicability of dynamic and continuous calibration across various transducer types. One of its core outcomes was to demonstrate the feasibility of applying dynamic and continuous calibration techniques at primary level, thereby laying the groundwork for future updates to international standards. The insights gained from ComTraForce supported emerging calibration protocols and contributed directly to the development of novel practices.

Additionally, the standardization effort led by ISO/TC 164/SC 1/SG 1 [7] has sought to translate these technical advances into normative documents. The subgroup's mandate includes defining terminology, calibration procedures, and uncertainty evaluation methods specifically tailored for continuous force calibration. Their work reflects a growing consensus on the need to extend metrological traceability beyond static loading, especially for applications involving fast-changing , such as, material characterization, component validation, and industrial automation.

Within this broader overview, the present study provides a comparative investigation of high-precision strain-gauge force transducers, with a capacity of 50 N, 100 N, 200 N and 500 N, following up the work

presented in [8]. The 200 N was calibrated under the three calibration modes (static, continuous, and dynamic), while all the other transducers were calibrated statically and dynamically. Using dedicated equipment and protocols corresponding to ISO 376, DKD-R 3-9, and DKD-R 3-10, the transducers are calibrated in compression. The aim is to assess consistency in sensitivity values, explore how uncertainty evolves under different loading regimes, and evaluate the compatibility of results across calibration types. In doing so, the study seeks to contribute to ongoing standardization efforts and support ISO/TC 164/SC 1/SG 1 and metrelogical community in defining best practices for traceable, application-relevant force calibration in both research and industrial contexts.

2. Materials and methods

2.1 Transducers under test

The experimental setup employs high-precision strain-gauge force transducers with nominal capacities of 50 N, 100 N, 200 N, and 500 N, manufactured by HBK (model TOP-Z30A), illustrated in Fig. 1. These devices are engineered to accurately measure small-scale tensile and compressive forces and are classified as Class 00 in accordance with ISO 376. Due to their high precision, the transducers are commonly employed as a reference standard in calibration systems or as transfer standards for machine verification in line with ISO 7500-1 [9]. They are interfaced with a 4 channels NI-9237 measurement amplifier (Fig. 2), which features a resolution of 0.00001 mV/V and connects via a 3-meter, 6-wire LAN-compatible cable. The amplifier is capable of simultaneously powering and reading up to four bridge-based sensors with six-wire configurations and ensures zero phase delay between measurement channels. Data is transmitted to a computer through an NI-9162 USB carrier and subsequently processed using LabView software.

Fig. 1. The 4 transducers under tests.

Fig. 2. NI-9237 measuring amplifier [8].

2.2 Static calibration according to ISO 376

The static calibration in compression of the tested force transducers was carried out in accordance with ISO 376, utilizing the INRiM 2.5 kN deadweight force standard machine. This calibration system has a declared Calibration and Measurement Capability (CMC) with a relative expanded uncertainty of 20 parts per million (ppm).

A sequence of ten evenly spaced force values, ranging from 10 % to 100 % of the transducers' capacity, was applied under both loading and unloading conditions. Each load step included a dwell period of at least 30 seconds and was repeated at three angular positions (0°, 120°, and 240°) as prescribed by the ISO standard. To reduce signal noise, a 0.1 Hz Bessel filter was implemented. The calibration included the evaluation of sensitivity and other transducer characteristics such as repeatability, reproducibility, resolution, hysteresis, return-to-zero behavior, and total relative expanded uncertainty for every 10% increment in force. Interpolation errors were not assessed, since the comparison was performed at each discrete load level (following ISO 376 Case B).

2.3 Continuous calibration according to DKD-R 3-9

The continuous calibration under compression of the 200 N transducer was conducted following the DKD-R 3-9 guideline, using the INRiM 1 kN continuous force calibration machine, illustrated in Fig. 3. This apparatus produces continuous forces via a stepper motor (Orientalmotor α-GRADE AR Series - AR HM 40093E 24DC), which drives a screw mechanism through a gearbox. Originally developed for polymer testing [10], the system was later characterized for its suitability in continuous calibration of force transducers.

The reference force was monitored using a 1 kN high-accuracy transducer (HBM Z3H3), installed at the base of the setup and connected to the same NI-9237 module described previously. This reference device was previously calibrated in compliance with DKD-R 3-9 Annex A [4], ensuring optimal measurement performance of the system during continuous loading. The applied correction factors and associated uncertainties, accounting for long-term drift, hysteresis effects, and transducer transfer behaviour, were established based on

the Annex A.4.2 procedure. The relative expanded uncertainty of the generated continuous reference force was determined to be 0.27%.

The loading sequence applied compressive forces up to the transducer's 200 N nominal capacity over a 120 s period, as recommended by the guideline. The trasducer was rotated by 120° steps around its axis. A 0.Hz Bessel filter was applied to both transducers, the reference and the one under test. Synchronicity of the two signals was guaranteed by the NI-9237 module, which simultaneously acquired both signals.

A ramp-type force-time profile was used, and data acquisition was performed at 25 Hz for both the reference and test transducers. Measurements were recorded during both loading and unloading phases. The evaluation of sensitivity, as well as key performance parameters, such as repeatability, hysteresis, reproducibility, and zero return, was carried out for ten force steps from 20 N to 200 N using the same procedures adopted during static calibration. Temperature effects were not considered, as all tests were performed in a thermally controlled environment at 21.0 ± 0.5 °C.

An example of what is obtained at two 0° repetition from the two transducers is depicted in Fig. 4. The non-perfect unloading ramp is due to the mechanical plug adapter behaviour, used primarily for materials tensile tests and adapted here for compression calibration. This impacted reversibility error, as shown in the following Section.

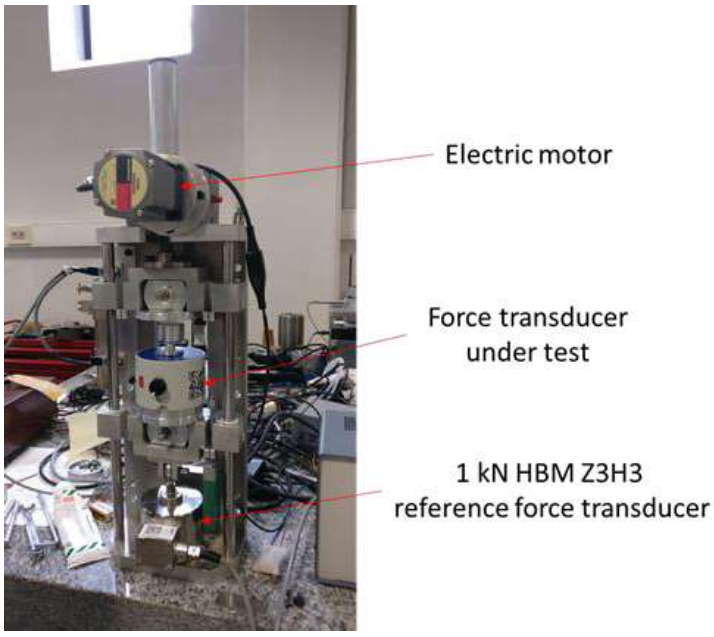

Fig. 3. The INRiM 1 kN continuous force calibration machine [8].

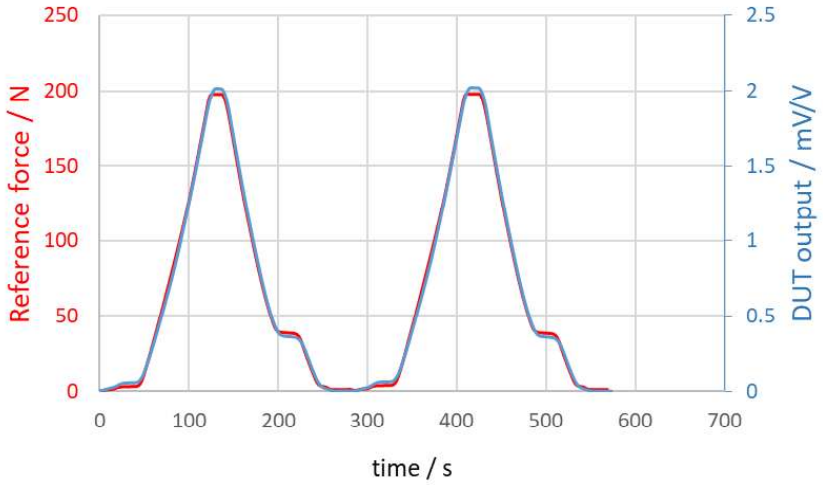

Fig. 4. Calibration output at 0° rotations from the reference transducer (red) and the 200 N transducer under test (blue).

2.4 Dynamic calibration according to DKD-R 3-10

The dynamic calibration of the transducers under test was performed in accordance with DKD-R 3-10 (Sheet 2), utilizing the INRiM primary vibration calibration system, as depicted in Fig. 5 [11,12]. This system comprises a vibrating platform (PCB model TMS 2075E), which is capable of generating sinusoidal oscillations up to 6000 Hz, and a Polytec OFV-5000 laser interferometer, employed to measure the acceleration of the loading mass, an essential parameter for determining dynamic force.

The setup includes several cylindrical test weights (210.67 g, 316.50 g, 422.44 g, and 528.88 g) that are mounted to the transducer during testing. To investigate resonance effects, an additional single-ended accelerometer is used to capture the motion of the vibrating base. Signal acquisition is facilitated by PCB 482C signal conditioners, as well as National Instruments NI 4431, NI 9162, and NI 9237 data acquisition modules. The latter has a flat frequency response within ±0.0025 dB [13] . Signals are acquired with a sampling rate of 5 kHz. Control of vibration frequency and amplitude is managed via LabView, while data analysis is carried out using MATLAB and Microsoft Excel.

For each calibration run, the force transducer's output (U_f) and the accelerations of both the loading mass (a_t) and the vibration platform (a_b) are recorded. As per DKD-R 3-10 [5], dynamic sensitivity is defined as the frequency-dependent ratio between the transducer's output signal U_f (in mV/V) and the actual dynamic force, which is computed by multiplying the total mass (external m_t plus internal mass of the transducer m_i) by the measured acceleration of the load a_t. This relationship is given in Eq. (1).

$$S_{\mathrm{dyn}} = \frac{U_{\mathrm{f}}}{(m_t + m_i)a_t} \tag{1}$$

Since this model assumes rigid body motion, deviations can occur due to elastic effects near the resonance frequency of the mass-spring system. In practice, the acceleration measured on the top surface of the load mass by the laser vibrometer may differ slightly from that of the base platform. To account for this elastic behavior, the dynamic sensitivity is also modeled using a second-order approximation recommended by DKD-R 3-10 [5], described in Eq. (2), with parameters p_1 and p_2 derived through linear regression on experimental sensitivity data across frequencies f.

$$S_{\mathrm{dyn,fit}} = p_1\left(1 - p_2 4\pi^2 f^2\right) \tag{2}$$

Prior to testing, the transducers' internal inertial mass m_i was determined using the method outlined in DKD-R 3-10 (§3.3.1) [5], yielding a value of approximately 122 g for each transducer. Calibration measurements were then conducted using all available weights, producing 91 sinusoidal force signals (30 seconds each) across the 10-100 Hz frequency range with a nominal amplitude of 2 m s^{-2}. U_f and a_t values correspond to the mean amplitudes computed by the software during the acquisition time. The generated dynamic force amplitudes ranged from approximately 0.7 N to 1.3 N, with maximum compressive forces, due to static load, reaching up to 6.4 N. Uncertainties for individual dynamic sensitivity values were calculated using the GUM framework (JCGM 100:2008) [14], considering the measurement uncertainties in mass, acceleration, transducer output, and internal mass determination. These were propagated using a Monte Carlo simulation (as per JCGM 101:2008 [15] and DKD-R 3-10 §3.4 [5]) to produce the uncertainty estimates for the model described in Eq. (2).

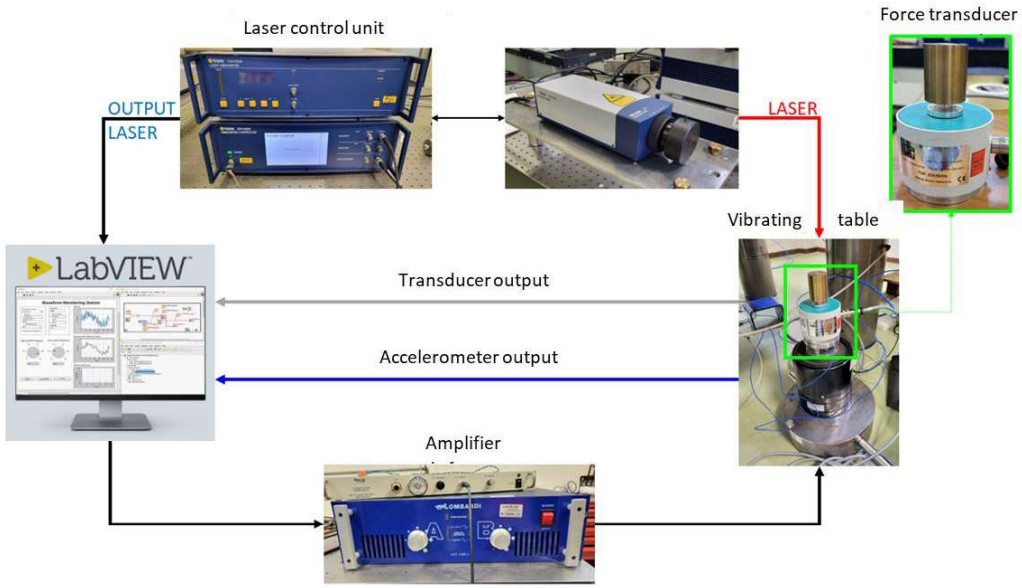

Fig. 5. INRiM dynamic force and vibration calibration system.

3. Results and discussion

3.1 Static calibration results

The static calibration outcomes from the tested transducers in terms of static sensitivity S_{stat} and relative expanded uncertainty $W(S_{\mathrm{stat}})$, as function of the ratio between the generated force F and the transducer's capacity F_{c}, obtained in compliance with ISO 376, are presented in Table 1. The force transducers satisfies the criteria for Class 00 performance for the whole force range. Across the entire calibrated force interval, the sensitivity values exhibit a high degree of consistency and stability, confirming the reliability of the transducer under static load conditions.

Table 1. Results according to ISO 376 in compression.

F/F_{c} / %	S_{stat} / (mV/V)/N				$W(S_{\mathrm{stat}})$ / %			
	50 N transducer	100 N transducer	200 N transducer	500 N transducer	50 N transducer	100 N transducer	200 N transducer	500 N transducer
10	0.039959	0.019996	0.010001	0.004002	0.020	0.014	0.010	0.003
20	0.039959	0.019995	0.010001	0.004002	0.015	0.010	0.004	0.004
30	0.039959	0.019995	0.010001	0.004002	0.013	0.006	0.004	0.004
40	0.039958	0.019994	0.010001	0.004002	0.012	0.007	0.003	0.004
50	0.039959	0.019994	0.010000	0.004002	0.013	0.006	0.003	0.003
60	0.039960	0.019994	0.010001	0.004002	0.012	0.006	0.003	0.003
70	0.039960	0.019994	0.010001	0.004002	0.011	0.006	0.003	0.003
80	0.039960	0.019993	0.010001	0.004002	0.011	0.006	0.003	0.003
90	0.039959	0.019993	0.010000	0.004002	0.011	0.006	0.004	0.003
100	0.039959	0.019993	0.010000	0.004002	0.011	0.006	0.002	0.003

3.2 Continuous calibration results

The compression-mode results for continuous calibration using a ramp force-time profile are provided in Table 2 for the 200 N transducer, with the uncertainty contribution mentioned in the reference guideline. The transducer's sensitivity S_{cont} response is generally linear across the measured range, though minor deviations from the static trend are observed at force levels of 40 N, 100 N, and 200 N. The increase in uncertainty, especially in the reversibility component, is attributed not only to the intrinsic behavior of the transducer under continuous loading, but also to imperfections in the mechanical coupling between the test and reference transducers. In particular, the non-ideal unloading ramp is likely due to the behavior of the mechanical plug adapter, originally designed for tensile tests and adapted here for compression calibration, as mentioned in the previous

Section. Similar patterns have been reported in earlier studies, such as those involving piezoelectric sensors [16].

Table 2. Results of the 200 N transducer under continuous loading according to DKD-R 3-9 with the ramp force time profile in compression mode.

F / N	S_{cont} / (mV/V)/N	w_{rep} / %	w_{rot} / %	w_{rev} / %	$W(S_{\mathrm{cont}})$ / %
20	0.00998	0.009	0.013	0.456	0.95
40	0.00988	0.002	0.007	0.222	0.52
60	0.01001	0.000	0.014	0.219	0.52
80	0.00999	0.001	0.013	0.341	0.73
100	0.00992	0.001	0.006	0.427	0.90
120	0.00999	0.001	0.004	0.535	1.10
140	0.00999	0.000	0.005	0.505	1.05
160	0.00999	0.000	0.006	0.435	0.91
180	0.01000	0.000	0.007	0.362	0.77
200	0.01005	0.000	0.011	///	0.27

3.3 Dynamic calibration results

The dynamic sensitivity of the force transducers under test as a function of both excitation frequency and applied loading mass, evaluated according to Eq. (1), is depicted in Fig. 6. As anticipated, sensitivity slightly decreases with increasing frequency. Minor fluctuations in the data can be attributed to resonance effects within the mechanical couplings rather than the primary mass-spring resonance of the system.

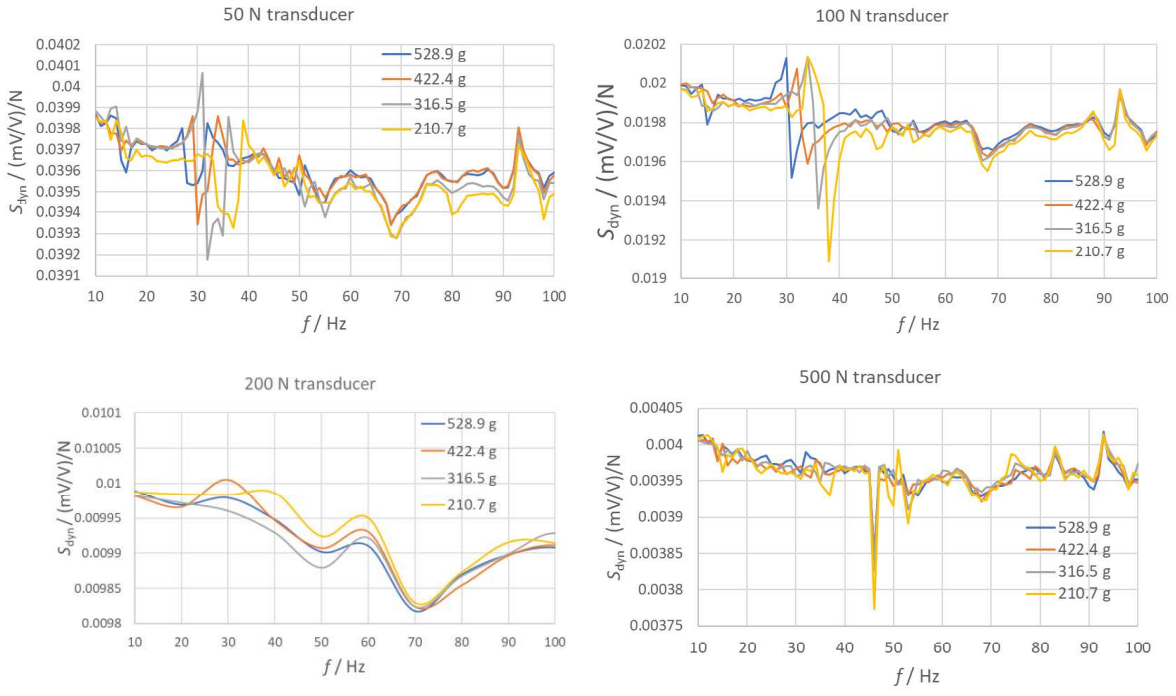

Fig. 6. Dynamic sensitivity as function of frequency and loading mass for the 4 transducers under test.

The associated relative expanded uncertainties of these values range from 0.1 % and 0.7 %, encompassing measurement uncertainties due to mass m_t (resolution of the mass balance), transducer signal output (resolution of the NI acquisition system), acceleration data (vibration calibration CMC at INRiM), and the internal mass estimation m_i (standard deviation of the fitting procedure). As an example, the expanded uncertainty associated with dynamic sensitivity for the 200 N trasducer with the 528.88 g loading mass at 10 Hz is reported in Table 3. $u^2(x_k)$ represents the variance of the individual uncertainty contributions (x_k), c_k is the sensitivity coefficient, $u_k^2(S_{dyn})$ is the variance of the dependent variable S_{dyn} due to the individual uncertainty contributions, and $U(S_{dyn})$ is the expanded uncertainty.

Table 3. Uncertainty budget (according to GUM) for S_{dyn} evaluated for the 200 N transducer with a loading mass of 528.9 at a frequency of 10 Hz.

	Variable x_k			$u^2(x_k)$	c_k	$u_k^2(S_{dyn})$
Symbol	Value	Meas. Unit	Note			
U_f	0.01305	mV/V	Type B	3.3E-11	7.7E-01	2.0E-11
a_t	2.0065	m s^{-2}	Type A	4.0E-06	-5.0E-03	1.0E-10
m_t	0.5289	kg	Type B	8.3E-12	-1.5E-02	2.0E-15
m_i	0.1222	kg	Type A	3.7E-07	-1.5E-02	8.8E-11
S_{dyn}	6.260			Variance, $u^2(S_{dyn})$		2.1E-10
				Exp. Unc. $U(S_{dyn})$		2.8E-05
				Rel. Exp. Unc. $W(S_{dyn})$		0.28 %

After that, experimental curves in Fig. 6 are fitted according to Eq. (2) using a Monte Carlo (MC) method. Probability density functions (PDFs), such as the normal distribution derived from uncertainty evaluation according to Table 3, are assigned to each experimental dynamic sensitivity as function of frequency. By utilizing the MC method, dynamic sensitivities are systematically sampled from their respective PDFs. This sampling allows for a Multiple Linear Regression (MLR) analysis to be performed according to Eq. (2). For each i-th MC iteration, MLR outputs are $p_{1,i}$and $p_{2,i}$ parameters together with their associated standard uncertainty from ordinary least squares (OLS), $u_{\mathrm{OLS}}(p_i)$. At the end of the MC iteration, N_{MC} iterations and regression planes, typically in the order of 10^6 to 10^7 as recommended in previous studies [17], are found. These regression planes are used to find the mean values of p_1 and p_2 (p, generally speaking) with associated standard deviations $u_{\mathrm{MC}}(c)$, as illustrated in Eqs. (3) and (4).

$$p = \frac{1}{N_{\mathrm{MC}}} \sum_{i=1}^{N_{\mathrm{MC}}} p_i \tag{3}$$

$$u_{MC}(p) = \sqrt{\frac{\sum_{i=1}^{N_{\mathrm{MC}}} (p_i - p)^2}{N_{\mathrm{MC}}(N_{\mathrm{MC}} - 1)}} \tag{4}$$

The total standard uncertainty of sensitivity coefficients is then determined by summing the squares of $u_{MC}(p)$ and $u_{OLS}(p)$, according to

$$u(p) = \sqrt{u_{MC}(p)^2 + u_{OLS}(p)^2} \tag{5}$$

where $u_{OLS}(p)$ is the mean standard uncertainty from the N_{MC} OLS given by

$$u_{OLS}(p) = \frac{1}{N_{MC}} \sum_{i=1}^{N_{MC}} u_{OLS}(p_i) \tag{6}$$

Expended uncertainty $U(p)$ is then determined by multiplying standard uncertainty $u(p)$ by 2. By propagating the uncertainties of p_1 and p_2 according to Eq. (2) model, the uncertainty associated with $S_{dyn,fit}$ can be obtained.

Table 4 summarizes the regression-derived parameters p_1 and p_2 for all tested transducers for all loading masses. p_1 values closely align with the static sensitivity across all masses, while p_2 coefficients vary depending on the attached load.

Fig. 7 displays the resulting model curves from which the decay of sensitivity as function of frequency is evident, while Fig. 8 compares, for example, experimental and modeled sensitivity curves for the 100 N transducer with the 422.4 g loading mass, showing how the model effectively smooths out irregularities caused by mechanical resonances.

Regarding the uncertainties, the OLS contributions dominate due to the variability of measurements near resonance zones. Uncertainty levels range from about 1% to nearly 8%, due to increasing signal dispersion and regression error.

Table 4. Values of p_1 and p_2 coefficients according to Eq. (2) as a function of the loading mass for the tested transducers.

m_t / g	p_1 / (mV/V)/N				p_2 / s^2			
	50 N transducer	100 N transducer	200 N transducer	500 N transducer	50 N transducer	100 N transducer	200 N transducer	500 N transducer
210.67	0.039638	0.019830	0.009912	0.003962	1.47E-08	1.88E-08	2.70E-09	2.99E-09
316.46	0.039674	0.019851	0.009935	0.003968	1.55E-08	1.73E-08	3.40E-09	6.22E-09
422.40	0.039677	0.019861	0.0099 37	0.003968	1.09E-08	1.91E-08	2.27E-09	9.44E-09
528.88	0.039669	0.019871	0.009954	0.003972	1.03E-08	1.92E-08	2.48E-09	1.59E-08

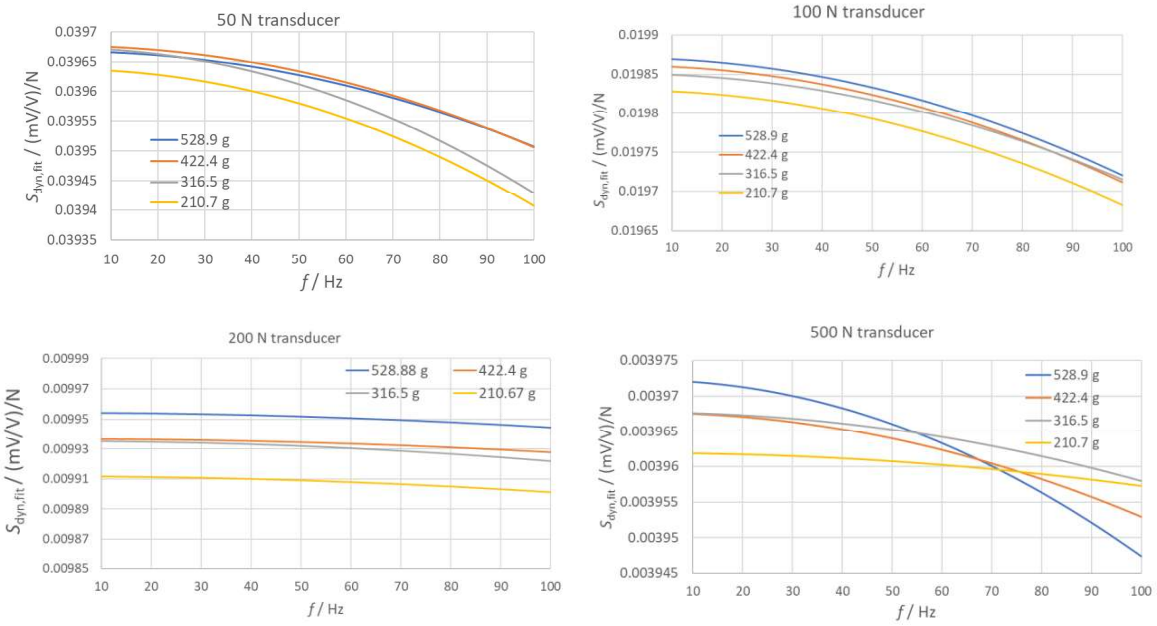

Fig. 7. Fitted dynamic sensitivity as function of frequency and loading mass for the 4 transducers under test.

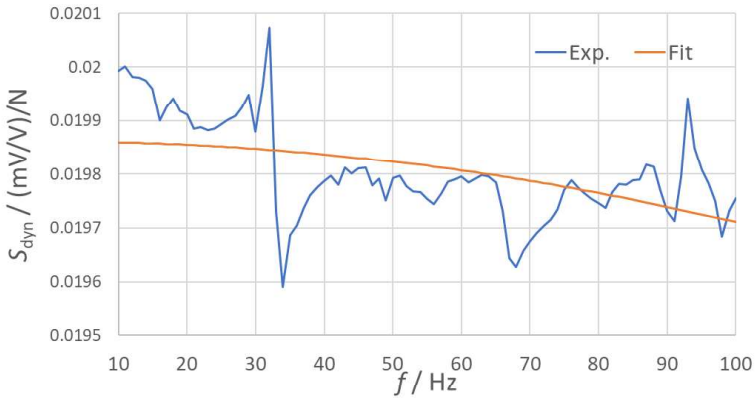

Fig. 8. Comparison between S_{dyn} and $S_{dyn,fit}$ curves for the 100 N transducer with the 422.4 g loading mass.

3.4 Comparison of Results from Different Calibration Methods

A comparison between static and continuous calibration results was first conducted for the 200 N transducer at overlapping force levels ranging from 20 N to 200 N. As illustrated in Fig. 9, the sensitivity values obtained from both methods are plotted alongside their respective expanded uncertainties. Although static calibration consistently yields lower uncertainties, both data sets show general agreement, with the exception of some deviations at 40 N and 200 N in the continuous case. A similar anomaly is observed at 100 N, though in that instance the associated uncertainty compensates for the discrepancy. These differences may stem from signal

instability in zero-point detection or from imperfections in the mechanical interface between the reference and test transducers.

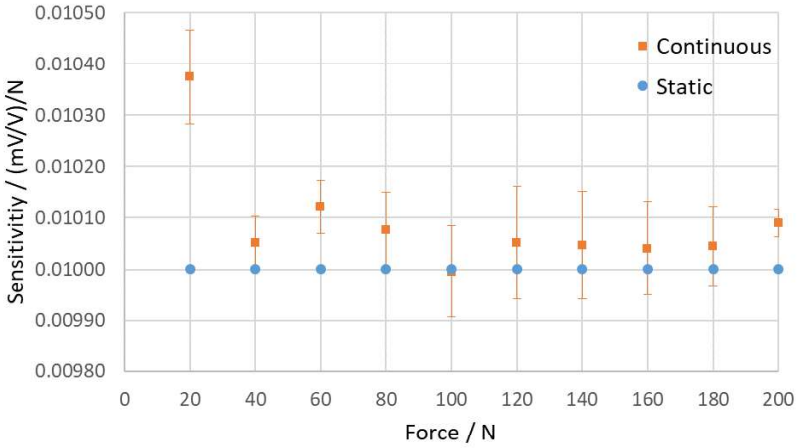

Fig. 9. Comparison between static and continuous calibration results of the 200 N transducer in terms of sensitivity as function of applied load [8].

To enable a broader comparison with the dynamic results, mean sensitivity values were calculated: 0.010001 (mV/V)/N for static and 0.009980 (mV/V)/N for continuous calibration. Expanded uncertainties for both means were computed using the root-sum-square of the average standard uncertainty and the standard deviation across all measured steps [18]. The resulting relative uncertainties were 0.030% and 0.772%, respectively.

Fig. 10 presents a comparative overview of static, continuous, and dynamic sensitivity values for the 200 N transducer. Notably, dynamic sensitivities trend lower than static and continuous ones. Anyway, compatibility is visually assessed using the uncertainty bands of the static and continuous sensitivities. For clarity, dynamic uncertainties (which range around 1% below 100 Hz) are omitted from the figure.

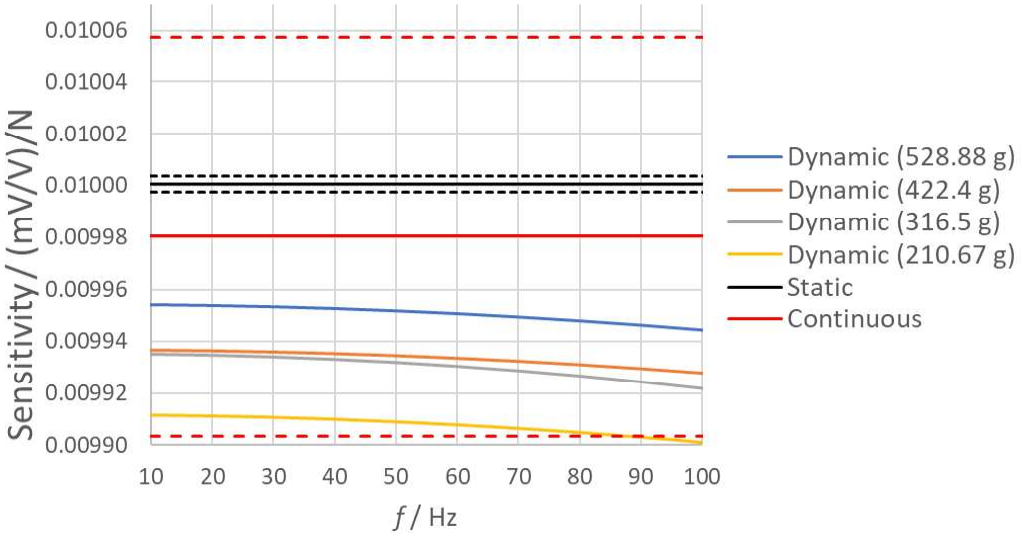

Fig. 10. Comparison between static, continuous and dynamic calibration sensitivities up to 100 Hz for the 200 N transducer. Dotted lines correspond to lower and upper limits of mean static and continuous sensitivities with associated expanded uncertainty [8].

Based on this comparison, the results from all three calibration regimes appear broadly compatible within their respective uncertainty bounds. However, this compatibility is highly sensitive to the declared uncertainty levels. If the uncertainties in dynamic and continuous calibrations were reduced to match those of static calibration, compatibility would likely be compromised due to the more pronounced discrepancies. Specifically, when using static calibration as a reference, continuous sensitivity shows closer agreement than dynamic sensitivity, which diverges more as the load decreases, an observation consistent with earlier findings [12]. This is also confirmed by comparing static and dynamic sensitivities for the other tested transducers as depicted in Fig. 11.

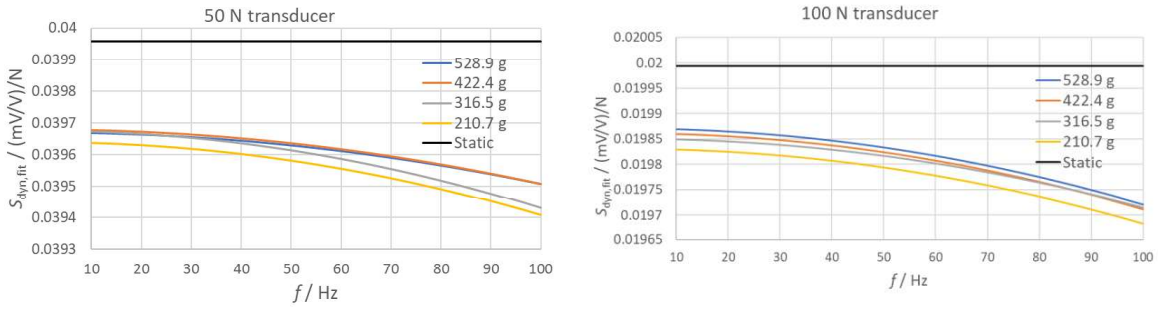

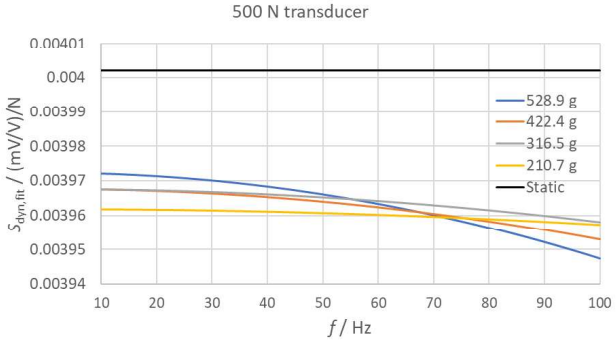

Fig. 11. Comparison between static and dynamic calibration sensitivities up to 100 Hz for the 50 N, 100 N and 500 N transducers.

Since dynamic values are given as function of frequency, the dynamic sensitivities extrapolated at f=0 Hz, i.e., p_1 values from Table 4, are also compared with static sensitivity from Table 1 in order to get a more robust comparison. For this purpose, relative differences as function of loading mass are calculated and depicted in Fig. 12 for all tested transducers.

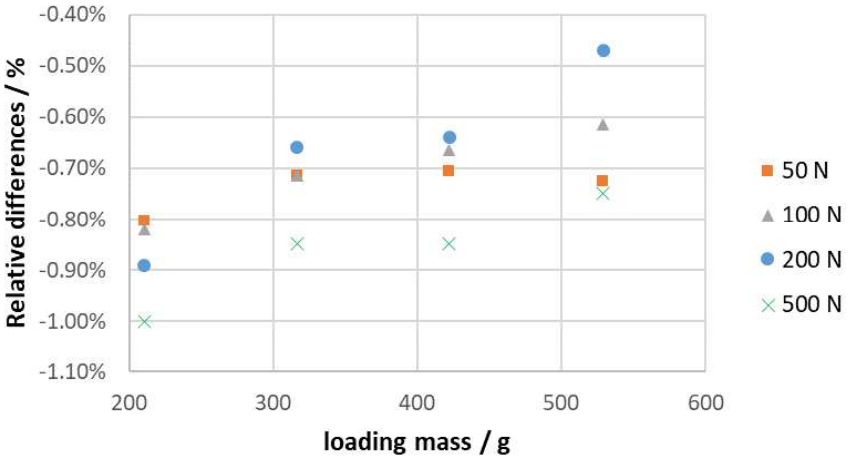

Fig. 12. Relative differences between dynamic sensitivity at f=0 Hz, i.e. p_1, and static one for the 50 N, 100 N, 200 N and 500 N transducers.

It is found that relative differences range between -1 % and -0.5 %, decreasing at increasing loading mass for all tested transducers. This may indicate that as the applied dynamic force deviates further from the transducer's nominal capacity, the dynamic sensitivity increasingly diverges from the static value, similarly to [19]. However, since dynamic calibration cannot currently reach force levels near the transducer's nominal limit, doubts remains about the true behavior of the transducer in those regions. This raises questions about the effectiveness of the dynamic calibration approach, despite its theoretical and metrological validity. In real-

world applications, such as fatigue testing, transfer transducers are often subjected to dynamic loads up to full capacity [20], which dynamic calibration methods currently struggle to replicate.

Similar concerns apply to the interpretation of uncertainty values. The significantly higher uncertainties observed under continuous and dynamic conditions may reflect either inherent transducer limitations or limitations of the current calibration methodology and equipment. For these reasons, all influencing factors should be carefully considered before the broader adoption and standardization of these new calibration methods.

4. Conclusions

This study presents a comprehensive comparison of static, continuous, and dynamic calibration methods applied to low-force strain-gauge transducers with capacities ranging from 50 N to 500 N. The static calibration results, performed according to ISO 376, showed high repeatability, minimal deviation across force steps, and low uncertainties, confirming the reliability of these transducers under standard calibration conditions.

Continuous calibration, carried out in compliance with DKD-R 3-9, exhibited sensitivity values comparable to static calibration, although with noticeably higher uncertainties, particularly in reversibility. These increased uncertainties were found to arise not only from the transducer's behavior under non-static loading but also from mechanical imperfections in the calibration setup, such as adapter compliance and connection misalignment.

Dynamic calibration, implemented following DKD-R 3-10, revealed a frequency-dependent decrease in sensitivity, as expected from theoretical models. Dynamic sensitivities were consistently lower than static ones and exhibited a stronger divergence at lower excitation forces. This divergence decreased as the applied load approached the nominal capacity of the transducer. However, due to the physical limitations of dynamic setups, such full-range loading is not achievable in practice, leading to uncertainty about the transducer’s true dynamic performance near its upper limit.

Despite these limitations, regression modeling using Monte Carlo methods showed that extrapolated zero-frequency dynamic sensitivities (p_1 values) are generally consistent with static sensitivities, particularly for larger loading masses. Nevertheless, dynamic and continuous calibration methods continue to produce higher uncertainty levels, ranging from 0.3 % to over 1 %, compared to the sub-0.05 % uncertainties typically achieved with static methods.

The results demonstrate broad compatibility between calibration methods within declared uncertainties. However, if the uncertainty levels in continuous and dynamic calibrations were reduced to match those of static calibration, the underlying differences in sensitivity would render the methods incompatible. This highlights a fundamental challenge in the metrological traceability of force measurements under realistic operating conditions.

Ultimately, while dynamic and continuous calibration procedures are conceptually robust and supported by standardization initiatives (e.g., DKD, ComTraForce project, and ISO/TC 164/SC 1/SG 1), their practical im-

plementation remains limited by methodological and technical constraints. Further research is needed to improve system performance, reduce uncertainty contributions, and ensure traceability under dynamic loading, particularly in applications like fatigue testing, where full-range dynamic calibration is crucial.

Funding statement

This work was supported by EURAMET [18SIB08 ComTraForce project funded by the EMPIR programme].

References

[1] N. Vlajic, A. Chijioke, Traceable calibration and demonstration of a portable dynamic force transfer standard, Metrologia, 54(4), 2017.

[2] T. Esward, S. Eichstädt, I. Smith, T. Bruns, P. Davis, P. Harris, Estimating dynamic mechanical quantities and their associated uncertainties: application guidance. Metrologia, 56(1), 2018.

[3] ISO 376:2011 — Metallic materials — Calibration of force-proving instruments used for the verification of uniaxial testing machines.

[4] DKD-R 3-9:2020 — Continuous calibration of force transducers according to the comparison method.

[5] DKD-R 3-10:2019 (Sheet 2) — Dynamic calibration of force transducers according to the sinusoidal method.

[6] https://www.ptb.de/empir2019/comtraforce/home/

[7] https://www.iso.org/committee/53554.html

[8] A. Prato, A. Improta, M. Di Lernia, S. Nobile, A. Facello, F. Mazzoleni, A. Germak, A. Schiavi, Static, continuous and dynamic calibration of force transducers: A comparative study on a low-force strain-gauge measuring device, Measurement: Sensors, 38, 2025.

[9] ISO 7500-1:2018 - Verification of static uniaxial testing machines —Part 1: Tension/compression testing machines — Calibration and verification of the force-measuring system.

[10] A. Schiavi, A. Prato, Evidences of non-linear short-term stress relaxation in polymers, Polymer Testing 59, 2017, pp. 220 – 229.

[11] A. Prato. F. Mazzoleni, A. Schiavi, Metrological traceability for digital sensors in smart manufacturing: calibration of MEMS accelerometers and microphones at INRiM, 2019 II Workshop on Metrology for Industry 4.0 and IoT (MetroInd4.0&IoT), 2019.

[12] A. Schiavi, A. Prato, F. Mazzoleni, G. D'Emilia, A. Gaspari, E. Natale, Calibration of digital 3-axis MEMS accelerometers: A double-blind «multi-bilateral» comparison, 2020 IEEE International Workshop on Metrology for Industry 4.0 & IoT, art. no. 9138215, pp. 542 – 547, 2020.

[13] https://www.ni.com/docs/en-US/bundle/ni-9237-getting-started/page/overview.html?srsltid=AfmBOopq1pUSD1sNIe67mxuT15FzcCj8X1L388pD2VRfrV3saL9tBeql

[14] JCGM 100:2008, Evaluation of Measurement Data — Guide to the Expression of Uncertainty in Measurement (GUM), Joint Committee for Guides in Metrology, Sèvres, France.

[15] JCGM 101:2008, Evaluation of measurement data — Supplement 1 to the "Guide to the expression of uncertainty in measurement" — Propagation of distributions using a Monte Carlo method. Joint Committee for Guides in Metrology, Sèvres, France.

[16] J. Sander, R. Kumme, Comparison of force measuring devices with static and continuous loading, Measurement: Sensors, Volume 18, 2021.

[17] P. Rizza, M. Murgia, A. Prato, C. Origlia, A. Germak, Determination of sensitivity coefficients and their uncertainties in Rockwell hardness measurement: a Monte Carlo method for multiple linear regression, Metrologia, 60(1), 2022.
DOI: https://doi.org/10.1088/1681-7575/aca334

[18] A. Prato, F. Mazzoleni, G. D'Emilia, A. Gaspari, E. Natale, A. Schiavi, Metrological traceability of a digital 3-axis MEMS accelerometers sensor network, Measurement, Volume 184, 2021.

[19] N. Vlajic, A. Chijioke, Traceable dynamic calibration of force transducers by primary means, Metrologia 53 S136, 2016.

[20] ISO 4965-1:2012 — Metallic materials — Dynamic force calibration for uniaxial fatigue testing — Part 1: Testing systems.

Acknowledgements

The authors would like to thank Alessio Improta, Matteo Piras, Michele Di Lernia and Salvatore Nobile from Politecnico di Torino and Fabrizio Mazzoleni from INRiM, for their support in experimental measurements and data analysis.